Loss of function of *def* selectively up-regulates Δ*113p53* expression to arrest expansion growth of digestive organs in zebrafish

Jun Chen,[1,5] Hua Ruan,[1,4,5] Sok Meng Ng,[1] Chuan Gao,[4] Hui Meng Soo,[1] Wei Wu,[1] Zhenhai Zhang,[1] Zilong Wen,[2] David P. Lane,[3] and Jinrong Peng[1,4,6]

[1]Laboratory of Functional Genomics, [2]Laboratory of Molecular and Developmental Immunology, [3]Laboratory of Control of p53 Pathway, Institute of Molecular and Cell Biology, Proteos, Singapore 138673; [4]Department of Biological Sciences, National University of Singapore, Singapore 117543

Transcription factor p53 forms a network with associated factors to regulate the cell cycle and apoptosis in response to environmental stresses. However, there is currently no direct genetic evidence to show if or how the p53 pathway functions during organogenesis. Here we present evidence to show that the zebrafish *def* (digestive-organ expansion factor) gene encodes a novel pan-endoderm-specific factor. A loss-of-function mutation in *def* confers hypoplastic digestive organs and selectively up-regulates the expression of Δ*113p53*, counterpart to a newly identified isoform of *p53* produced by an alternative internal promoter in intron 4 of the *p53* gene in human. The increased Δ*113p53* expression is limited to within the mutant digestive organs, and this increase selectively induces the expression of p53-responsive genes to trigger the arrest of the cell cycle but not apoptosis, resulting in compromised organ growth in the mutant. Our data demonstrate that, while induction of expression of p53 and/or its isoforms is crucial to suppress abnormal cell growth, Δ*113p53* is tightly regulated by an organ/tissue-specific factor Def, especially during organogenesis, to prevent adverse inhibition of organ/tissue growth.

[*Keywords*: Def (digestive-organ expansion factor); endoderm organogenesis; p53; zebrafish]

Supplemental material is available at http://www.genesdev.org.

Received August 18, 2005; revised version accepted September 27, 2005.

In a normal cell, levels of p53 increase rapidly following stresses such as UV treatment and ionizing radiation (Levine 1997). An increase in the level of p53 in response to environmental stresses will both initiate and suppress the expression of target genes to regulate cell cycle and cell death in order to eliminate abnormal, potentially cancer-predisposing cells and to maintain genome stability (Vogelstein et al. 2000; Schumacher et al. 2005). This property makes *p53* a well-known tumor-suppressor gene (Greenblatt et al. 1994). However, there is little genetic evidence to show if p53 is necessary for organogenesis during embryogenesis. Studies of loss-of-function mutants in mouse, zebrafish, *Drosophila*, and *Caenorhabditis elegans* showed that all p53 mutants suppressed stress-induced (e.g., radiation) apoptosis, and, in the case of mouse and zebrafish, mutants were also susceptible to developing tumors. Further detailed studies showed that a subset of embryos of $p53^{-/-}$ female mice displayed defects in neural tube closure resulting in overgrowth of neural tissue in the region of the mid-brain, a condition known as exencephaly (Armstrong et al. 1995; Sah et al. 1995). Otherwise, in general, p53 mutants were viable and did not confer other obvious developmental defects during embryogenesis (Donehower et al. 1992; Jin et al. 2000; Ollmann et al. 2000; Derry et al. 2001; Berghmans et al. 2005). In contrast, overexpression of p53, either ectopically or in transgenic animals, caused various developmental abnormalities. Ectopic overexpression of *Drosophila* Dmp53 in the eye caused cell death and led to a rough and small eye phenotype (Jin et al. 2000; Ollmann et al. 2000). Overproduction of *C. elegans* p53 (CEP-1) in the *GLD-1* mutant, which encodes a translational repressor of CEP-1, led to the elevation of p53-mediated germ cell apoptosis in response to DNA damage (Schumacher et al. 2005). In mouse, loss of function of *mdm2* caused embryonic lethality, while $mdm2^{-/-}$ $p53^{-/-}$ double-mutant mice developed normally, suggesting that the activity of p53 in $mdm2^{-/-}$

[5]These authors contributed equally to this work.
[6]Corresponding author.
E-MAIL pengjr@imcb.a-star.edu.sg; FAX 65-67791117.
Article and publication are at http://www.genesdev.org/cgi/doi/10.1101/gad.1366405.

embryos is the likely cause of lethality (Montes de Oca et al. 1995). In zebrafish, increase in p53 by knock-down of *mdm2* using *mdm2*-specific morpholinos caused severe developmental arrest during embryogenesis. Coinjection of *p53*-specific morpholinos rescued the morphant phenotype to normal (Langheinrich et al. 2002). Apparently, an organism has to develop systems to keep p53 at a low level to protect normal development. In fact, although p53 is ubiquitously expressed, the p53 protein is kept at low levels in normal cells by Mdm2, an E3 ligase that targets p53 for degradation via the ubiquitin-mediated 26S proteasome pathway (Momand et al. 1992). In addition, the fact that p53 shows cell-autonomous haploinsufficiency implies that p53 transcription must be also very tightly regulated to ensure the correct activity of the p53 pathway (Clarke et al. 1993). However, very little is known about if or how p53 expression, especially at the transcription level, is regulated in a specific organ/tissue during organogenesis. Furthermore, it has very recently been shown that p53, as found for p63 and p73, exists in multiple isoforms derived from either alternative splicing or products initiated by an alternative promoter (Benard et al. 2003; Melino et al. 2003; Bourdon et al. 2005). One of the *p53* isoforms, Δ*133p53*, is derived from an alternative promoter in intron 4 of *p53* gene. However, little is known about how Δ*133p53* expression is regulated and what kind of biological function it plays. In mice expressing an N-terminally truncated fragment of p53 as well as the full-length protein, an accelerated aging phenotype has been reported that seems to be due to excess activation of p53 function (Tyner et al. 2002), whereas in transfection-based systems, such truncated fragments can act as dominant-negative inhibitors of p53 (Bourdon et al. 2005).

The vertebrate alimentary tracts are derived from a common primitive gut tube that originates from the endodermal layer (Wells and Melton 1999). In mammals, the primitive gut tube is defined into fore-, mid-, and hindgut regions (Kiefer 2003). The liver, lung, thyroid, and the ventral rudiment of the pancreas are all originated from the ventral foregut endoderm, while the esophagus, stomach, dorsal pancreas, and duodenum arise from the dorsal endoderm of the foregut and midgut (Wells and Melton 1999; Edlund 2002; Zaret 2002; Horne-Badovinac et al. 2003; Ober et al. 2003). In zebrafish, endodermal progenitor cells are located around the margin, the region where the blastoderm meets the yolk cells at the yolk syncytial layer (YSL) at the mid-blastula stage, and begin to involute during gastrulation. The endodermal cells then form a sparse but uniform monolayer by the end of gastrulation (10 h post-fertilization [hpf]) (Warga and Nusslein-Volhard 1999). Later, endodermal cells move medially to form a solid rod that gives rise to the endodermal components of the alimentary canal and its derived organs, such as liver, gallbladder, pancreas, and swimbladder (Field et al. 2003; Ober et al. 2003; Wallace and Pack 2003; Wallace et al. 2005). By 50 hpf, both liver and pancreatic buds become obvious organs connected to the gut tube (Field et al. 2003; Ober et al. 2003; Wallace and Pack 2003).

Although several factors have been identified as master controls for the initiation, development, and differentiation of digestive organs, very little is known about how the fundamental mechanisms of cell division, growth, and movement are coordinated with these specific factors to control the development of digestive organs to reach the final size, shape, and position in the body. In this report, we present our studies on the *def* (digestive-organ expansion factor) gene and the *def*^{hi429} mutant in zebrafish. The expression of *def* is enriched in the digestive organs at the later stage of organogenesis. Histological analysis and in situ hybridization showed that the initiation and early development of digestive organs are not obviously altered in the *def*^{hi429} mutant. However, at a later stage, all digestive organs display hypoplasia. Studies using organ-specific markers showed that cell differentiation does occur but organ expansion and maturation are compromised in the mutant. Surprisingly, detailed studies showed that the expression of Δ*113p53*, a counterpart to the human isoform Δ*133p53* initiated by an alternative promoter in intron 4 (Bourdon et al. 2005), is selectively up-regulated in the *def*^{hi429} mutant. More interestingly, this increase in Δ*113p53* expression was restricted within the mutant endoderm organs, and this expression pattern phenocopies the expression pattern of the wild-type *def* gene. The increased level of Δ*113p53* induces the expression of p53 response genes and causes obvious arrest of cell proliferation in the mutant digestive organs from 3 d post-fertilization (dpf). Thus, Def acts as a pan-endoderm factor to coordinate the expansion growth of the entire digestive system through negatively regulating Δ*113p53* expression in zebrafish.

Results

Major digestive organs in the def^{hi429} *mutant are severely hypoplastic*

The hi429 line was originally identified through screening progenies derived from retrovirus insertional mutagenesis (Golling et al. 2002) and was outcrossed three times with the wild-type progenitor AB^{tü} before used for characterization in this study. The homozygous mutant appeared normal up to 3 dpf. At 5.5 dpf, the mutant fish could be easily distinguished from other siblings by showing a large unabsorbed yolk (Fig. 1A,B). In addition, the mutant fish had an underexpanded anterior intestine and a smaller liver, pancreas, and swimbladder when viewed under a dissecting microscope (Fig. 1A,B). Phenol Red injection showed that, in addition to the defects observed for the intestine, the gallbladder was also smaller in size in the mutant fish (Fig. 1C,D). In zebrafish, there are seven pairs of branchial arches along the mouth that are derived from the endoderm (Neuhauss et al. 1996). In the *hi429* mutant, branchial arches 2–7 are reduced in size and the cartilage has an irregular shape compared with the wild type (Fig. 1E,F). The mutant dies between 8 and 11 dpf. On the other hand, alkaline phosphatase (AP) staining showed that the development of pronephric

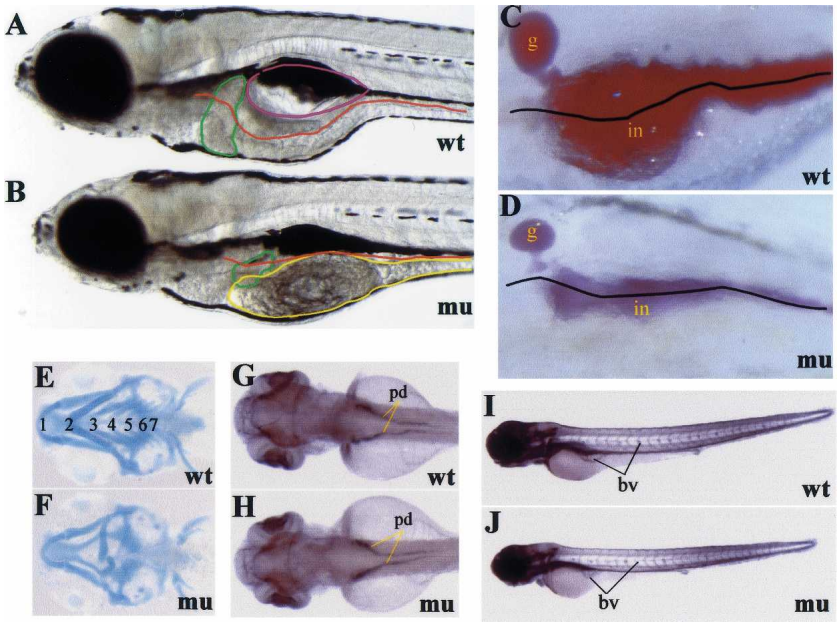

Figure 1. The *def*^{hi429} mutant exhibits hypoplastic digestive organs. (*A*,*B*) At 5.5 dpf, the *def*^{hi429} mutant had an unabsorbed york sac and exhibited smaller liver and swimbladder and much thinner intestine as seen by dissection microscopes. The liver is outlined with green, the gut with red, the swimbladder with purple, and the york sac with yellow. (mu) Mutant; (wt) wild-type. (*C*,*D*) At 5 dpf, Phenol Red injection revealed that the *def*^{hi429} mutant had a smaller gallbladder (g) and underexpanded anterior intestine (in). The gut from anterior to posterior (*left* to *right*) is outlined with a black line. (*E*,*F*) At 5 dpf, alcian blue staining showed that the branchial arches 2–7 in the *def*^{hi429} mutant (mu) were deformed. Branchial arches 1–7 in wild type are indicated in *E*. (*G*–*J*) Histochemical staining of alkaline phosphatase showed that pronephric ducts (*G*,*H*) at 3 dpf and blood vessels (*I*,*J*) at 4 dpf in wild type (wt) and the *def*^{hi429} mutant (mu) were indistinguishable. (bv) Blood vessels; (pd) pronephric ducts.

ducts at 3 dpf (Fig. 1G,H) and blood vessels at 4 dpf (Fig. 1I,J), two mesoderm-derived organs, appeared normal in the mutant. Other unaffected structures and organs include somites and body size (Fig. 1B,J). These results suggest that the main function of the wild-type gene product is limited to the digestive organs. Because *hi429* exhibits hypoplasia in the digestive organs, we renamed this gene as *def*, and the mutant is designated as *def*^{hi429}.

Def is essential for the intestine expansion growth but not the endoderm–intestine transition

Examination of expression of the early endoderm markers *foxa1* (Fig. 2A,B), *foxa3*, and *shh* (data not shown) did not reveal discernible differences between mutant and wild-type embryos before 2 dpf, suggesting that *def* might not play a major role during the early stage of endodermal organogenesis. In the zebrafish, the endoderm–intestine transition happens ~60 hpf and is marked morphologically by the formation of columnar epithelium with highly organized brush border microvilli and molecularly by expression of gut-specific proteins such as intestine fatty acid-binding protein (ifabp) and AP (Mayer and Fishman 2003). Transmission electron microscope (TEM) analysis revealed that the mutant intestine tube did form a columnar epithelium and brush border (data not shown). However, the mutant anterior intestine tube was underexpanded, and the columnar epithelium did not fold properly, likely due to a greatly reduced number of epithelial cells (Fig. 2C,D). Whole-mount in situ hybridization and histochemical assay showed that, although at much lower levels when compared with the wild type, both *ifabp* (Fig. 2E,F) and AP (Fig. 2G,H) are expressed in the mutant intestine. Based on these results, it seems that the *def*^{hi429} mutation does not abolish cell differentiation but mainly affects organ growth/expansion.

Def is required for expansion growth of the exocrine but not the endocrine pancreas

The zebrafish pancreas originates from two anlagen, the first (posterior one) initiating at ~24 hpf and the second (anterior one) at ~40 hpf. These two buds merge at 52 hpf to form the morphologically identifiable pancreas (Field et al. 2003; Ober et al. 2003). *pdx1* staining did not reveal discernible defects in the *def*^{hi429} mutant at 2 dpf, suggesting that *def* is not essential for the initiation and budding of the pancreas (Fig. 2I,J). Whole-mount in situ hybridization using the exocrine pancreas-specific marker *trypsin* showed that the mutant pancreas did express *trypsin*; however, the size of exocrine pancreas marked by *trypsin* expression was significantly smaller than that in the wild type at 3 dpf (Fig. 2K,L). In contrast, examination of the expression of *insulin*, an endocrine pancreas-specific marker, revealed that the islet size and signal intensity of *insulin* in mutant fish were indistinguishable from that in the wild type (Fig. 2M,N). Histological sectioning and in situ hybridization clearly showed that the mutant pancreatic islet appeared normal; however, it was surrounded only by a thin layer of exocrine cells that clearly expressed *trypsin* (Fig. 2O,P). This observation suggests that *def* regulates the expansion growth of exocrine pancreas rather than the process of cell differentiation.

Def is required for liver expansion growth

The wild-type zebrafish liver bud appears at ~44 hpf (Ober et al. 2003; Wallace and Pack 2003) and undergoes rapid expansion to form the left and right two lobes between 3 and 5 dpf (Mayer and Fishman 2003). Examination of liver development using *prox1* as marker did not reveal discernible differences between the *def*^{hi429} mutant and wild type up to 2 dpf (Fig. 2Q,R), suggesting that *def* is not essential for the initiation and budding of liver.

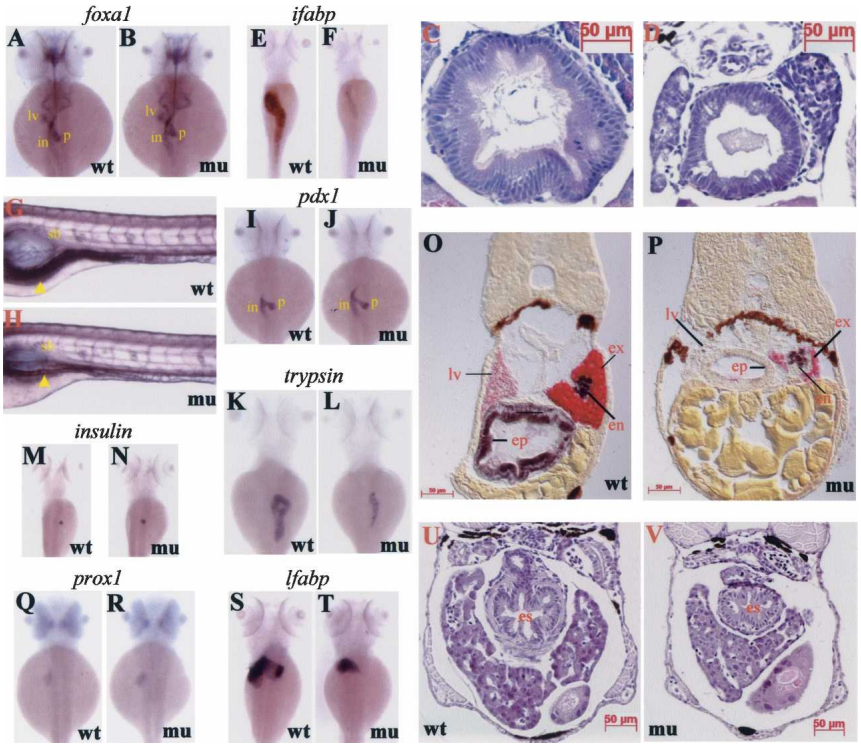

Figure 2. *def* is required for the expansion growth of intestine, liver, and exocrine pancreas but not endocrine pancreas. (*A*,*B*) At 2 dpf, whole-mount in situ hybridization using the pan-endoderm marker *foxa1* showed that there were no discernible phenotypic differences between wild type (wt) and *def*^{hi429} mutant (mu). (in) Intestine; (lv) liver; (p) pancreas. (*C*,*D*) At 5 dpf, cross-sectioning showed that the columnar epithelium did form in the mutant gut (mu) but did not fold properly obviously due to greatly reduced cell number when compared with the wild type (wt). (*E*–*H*) The expression of gut-specific markers *ifabp* at 4 dpf (*E*,*F*) and alkaline phosphatase at 5 dpf (*G*,*H*, yellow arrows) was greatly reduced in the *def*^{hi429} mutant. (mu) Mutant; (sw) swimbladder; (wt) wild type. (*I*,*J*) At 2 dpf, whole-mount in situ hybridization using a *pdx1* probe showed that the initiation and formation of pancreatic bud (p) was not affected in the *def*^{hi429} mutant (mu). (in) Intestine. (*K*,*L*) At 3 dpf, whole-mount in situ hybridization using a *trypsin* probe showed that the *def*^{hi429} mutant exhibited a much smaller exocrine pancreas. (*M*,*N*) In contrast, at 4 dpf, whole-mount in situ hybridization using an *insulin* probe showed that the endocrine pancreas had no discernible difference between the *def*^{hi429} mutant (mu) and the wild type (wt). (*O*,*P*) At 4.5 dpf, sectioning in situ hybridization using Fast Red (Roche)-labeled *trypsin* (for exocrine pancreas, in red) and DIG-labeled *insulin* (for endocrine pancreas, in purple) probes further confirmed that, when compared with the wild type (wt), the mass of the exocrine pancreas (ex) was greatly reduced while the endocrine pancreas (en) appeared normal in the *def*^{hi429} mutant (mu). The mutant epithelium (ep) was narrower and only weakly expressed *ifabp* (in purple). The liver (lv) in the wild type was labeled using a *transferrin* probe (for liver, red). (*Q*,*R*) At 2 dpf, whole-mount in situ hybridization using *prox1* did not reveal a discernible difference between the *def*^{hi429} mutant (mu) and the wild type (wt). (*S*,*T*) At 4 dpf, the liver bud was obviously smaller and failed to form two lobes in the *def*^{hi429} mutant. (*U*,*V*) At 5 dpf, cross-sectioning through the esophagus (es) revealed that bile ducts and blood vessels were properly formed in the *def*^{hi429} mutant liver (mu) as in the wild-type liver (wt).

However, the mutant liver was arrested as an oblong-shaped bud on the left side and failed to form the left and right two lobes at 4–5 dpf (Fig. 2S,T). Although its expansion growth was severely retarded, the mutant liver clearly expressed *lfabp*, suggesting that the differentiation of hepatocytes is not blocked in the *def*^{hi429} mutant (Fig. 2S,T). In fact, histological sectioning showed that bile ducts and blood vessels were clearly visible in the mutant liver (Fig. 2U,V). These data demonstrate that the *def*^{hi429} mutation mainly affects the expansion growth of liver but does not alter the differentiation of hepatoblast to hepatocytes and bile duct cells.

def mRNA rescued the mutant phenotype

Molecular analysis showed that the viral vector is inserted within the second intron of the *def* gene (Fig. 3A; Golling et al. 2002). We obtained a full-length *def* cDNA clone via an RT–PCR method and confirmed that *def* encodes a novel protein of 753 amino acids. BLAST searches revealed that Def has homologs in human, mouse, *Drosophila*, and yeast, with highest homology with human (51% identity) and mouse (52% identity) counterparts of yet unknown function (Fig. 3B). Sequencing the genomic DNA fragment containing the *def* gene showed that the *def* gene contains 13 exons spanned by 12 introns (Fig. 3A).

Initial reports indicated that the *def*^{hi429} mutant phenotype cosegregated with the insertion site (Golling et al. 2002). To confirm the linkage between the *def*^{hi429} mutation and the mutant phenotype, a total of 588 embryos from five pairs of *def*^{hi429} heterozygote crosses were genotyped, and we found that only individuals homozygous for the viral vector insertion (157 out of 588) displayed the mutant phenotype, suggesting that the mutant phenotype is closely linked to the viral vector insertion. To unequivocally prove that the mutant phenotype is caused by the viral vector insertion, *def* wild-type mRNA was obtained from the in vitro transcription of the full-length cDNA and was injected into one-cell-stage embryos. At 3 dpf, 69% of the mutants injected with *def* mRNA (42 out of 61) had the expression of *ifabp* restored and 15% (nine out of 61) were partially rescued, accounting for 84% of total mutant embryos examined (Fig. 3C). At 4 dpf, 62% of the mutants injected with *def* mRNA (28 out of 45) developed a normal exocrine pan-

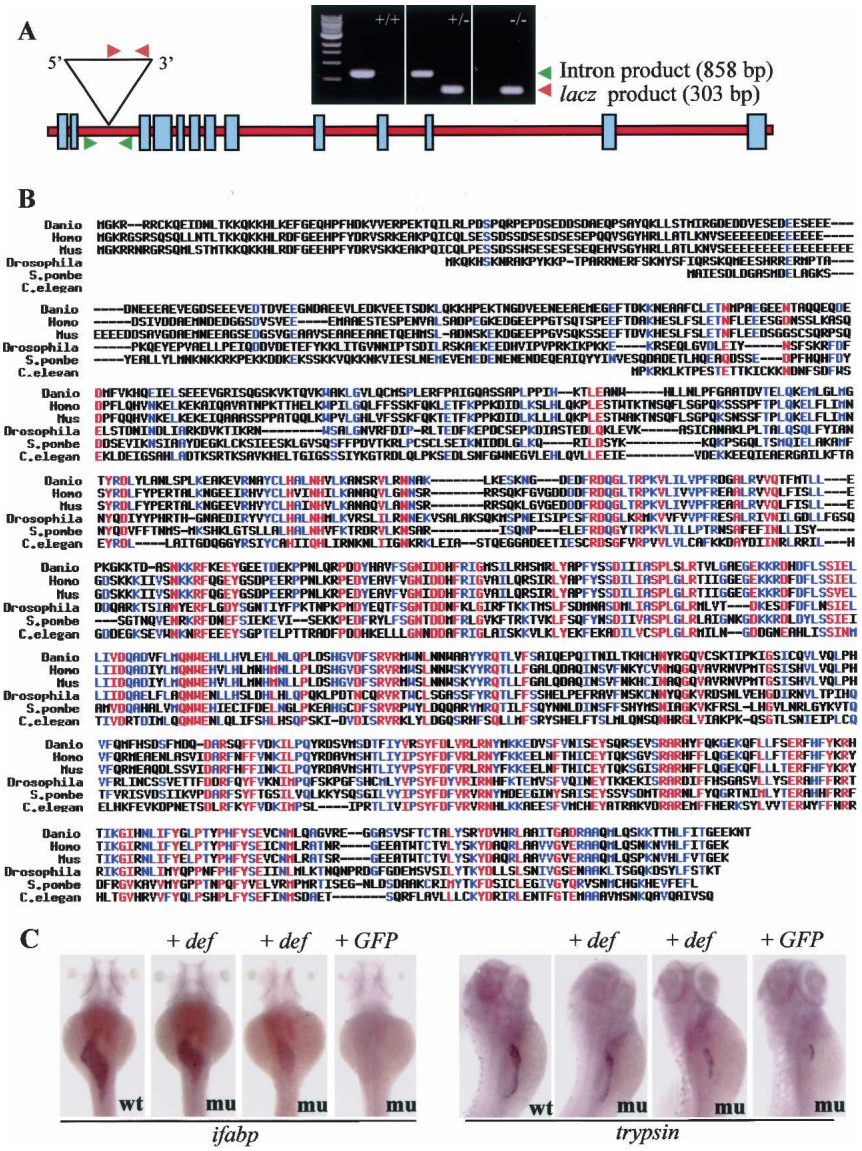

Figure 3. Viral vector insertion in the *def* gene caused the *def*^{hi429} mutant phenotype. (*A*) Schematic drawing shows the genomic DNA structure of the *def* gene. The viral vector was inserted in the second intron. The positions of two pairs of primers used for genotyping the mutant embryos are indicated, and their PCR products are shown in the DNA gel photos, respectively. Red arrowheads represent the primer pair for checking the viral insertion in heterozygous (+/−) or homozygous (−/−) mutants; green arrowheads for checking the wild-type gene in wild-type sibling (+/+) or heterozygous mutant (+/−). (*B*) Amino acid sequence alignment of Def (gi37046654) and its homologs/orthologs in human (gi7657019), mouse (gi20340985), *Drosophila* (gi20130323), *C. elegans* (gi17555844), and yeast (gi19076047). (*C*) Injection of *def* mRNA (*def*) rescued the *def*^{hi429} mutant phenotype, whereas injection of *GFP* mRNA (*GFP*) or mutant *def*^{stop} mRNA (data not shown) failed to rescue the mutant phenotype. Embryos 3 and 4 d post-injection were used for whole-mount in situ hybridization with *ifabp* and *trypsin* probes, respectively. (mu) Mutant; (wt) wild-type.

creas and 24% (11 out of 45) were partially rescued, accounting for 86% in total, as revealed by checking *trypsin* expression (Fig. 3C). On the other hand, both *GFP* mRNA (135 injected mutant embryos examined) and a mutant form of the *def* gene (*def*^{stop}) with a G-T substitution converting GAA (Glu 55) to TAA (stop codon) (138 injected mutant embryos examined) failed to rescue the mutant phenotype. These results confirm that the viral insertion in the *def* gene caused the *def*^{hi429} mutant phenotype. Furthermore, the transcript of *def* was undetectable in the *def*^{hi429} mutant in RNA gel blot hybridization (Fig. 4A), strongly suggesting that the *def*^{hi429} mutant is likely a null allele.

def encodes a nuclear-localized protein and is enriched in the digestive organs

RNA gel blot hybridization showed that *def* has two isoforms, and both forms are expressed at comparable levels in unfertilized eggs and during the early stage of embryogenesis (Fig. 4A). However, in the adult liver, the short isoform is more abundant (Fig. 4A). The expression of *def* peaked in the embryos at 12 hpf and 1 dpf and was at high levels at 3 dpf and 4 dpf but decreased to a lower level at 5 dpf (Fig. 4A). To investigate the cellular localization of the Def protein, immunostaining was performed using anti-Def antibody, and the result showed that the Def protein is localized nuclearly (Fig. 4B). As described above, digestive organs in the *def*^{hi429} mutant exhibited hypoplasia, while ectoderm- and mesoderm-derived organs appeared relatively normal. The expression pattern of *def* was investigated via whole-mount and cross-section in situ hybridization. Whole-mount in situ hybridization showed that, at 2 dpf, *def* was ubiquitously expressed but was notably enriched in the mid- and hindbrain boundary (Fig. 4C). Through 3–5 dpf, the expression of *def* was more specifically enriched in the gut, liver, pancreas, and pharynx (Fig. 4D–F). Sectioning

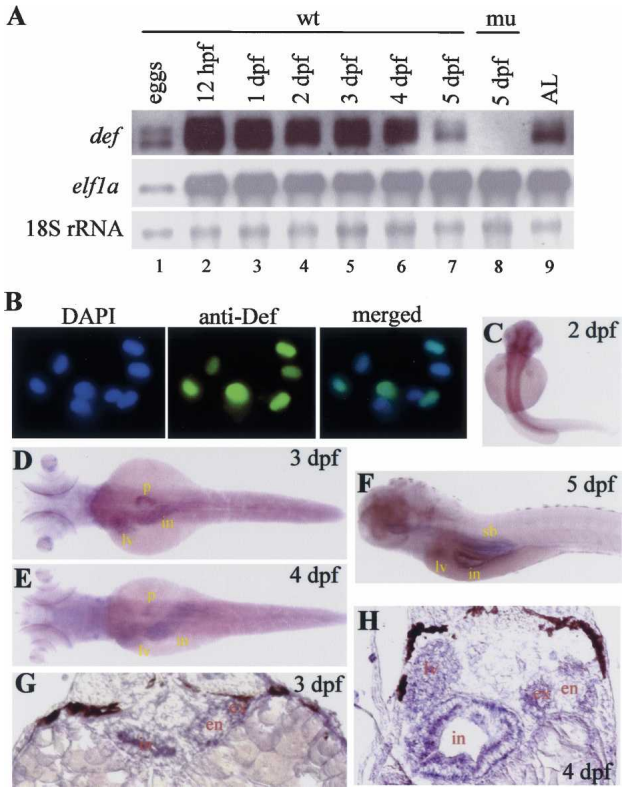

Figure 4. *def* encodes a nuclear protein, and its expression is enriched in the endoderm organs. (*A*, *top* panel, lanes *2–7*) RNA gel blot hybridization revealed that *def* had two transcribed forms that peaked at 12 hpf and 1 dpf and then gradually reduced to a lower level at 5 dpf. (Lane *9*) The shorter form was more abundant in the adult liver (AL). (Lane *8*) *def* expression is undetectable in the *def*^{hi429} mutant. (*elf1a*) *elongation factor 1a*. (*B*) Immunostaining using anti-Def antibody showed that Def is a nuclear-localized protein. (*C–F*) Whole-mount in situ hybridization using a *def* riboprobe to examine the expression patterns of *def* at 2 dpf (*C*), 3 dpf (*D*), 4 dpf (*E*), and 5 dpf (*F*). *def* expression was specifically enriched in the digestive organs from 3 to 5 dpf. (in) Intestine; (lv) liver; (p) pancreas; (sw) swim-bladder. (*G,H*) Sectioning in situ hybridization showed that *def* expression is specifically enriched in the intestine (in), liver (lv), and exocrine pancreas (ex) but is excluded from the endocrine pancreas (en) at 3 and 4 dpf.

in situ hybridization confirmed that *def* expression was specifically enriched in the liver, gut, and exocrine pancreas but was excluded from the islet (Fig. 4G,H). This expression pattern coincides with the observation that islet development is not affected in the *def*^{hi429} mutant (Fig. 2M,N).

Expression of Δ113p53 *but not the wild-type* p53 *is drastically up-regulated in the mutant digestive organs*

To identify genes downstream of *def*, RNA samples were prepared from wild-type and mutant whole fish, respectively, and were used to compare the expression profiles between the wild type and the *def*^{hi429} mutant at 5 dpf using the Affymetrix zebrafish GeneChip carrying 14,900 unigenes. Analysis of results obtained from five independent hybridizations showed that the expression of 141 genes was down-regulated at least twofold in the *def*^{hi429} mutant compared with the wild type (Supplementary Table 1). Extensive database search revealed that 122 of these down-regulated genes each can be assigned a biochemical function and the majority of them are well-known for their relative specific expression in digestive organs (Supplementary Table 1). On the other hand, only 23 genes are specifically up-regulated (greater than or equal to twofold) in the *def*^{hi429} mutant (Supplementary Table 2). Surprisingly, the tumor-suppressor gene *p53* and its response genes *mdm2* and *cyclin G1* are among these 23 up-regulated genes (Supplementary Table 2).

To confirm the result obtained from the microarray hybridization, RNA gel blot hybridization was performed to compare the *p53* transcripts in the *def*^{hi429} mutant and wild-type control. In the wild type, *p53* expression peaks at 1 dpf, then decreases gradually to a lower level at 5 dpf (Supplementary Fig. S1A). Surprisingly, at 5 dpf, a short form of *p53* transcripts in the *def*^{hi429} mutant showed very high levels, whereas this short form was almost undetectable in the wild-type embryos from 1 dpf to 5 dpf (Supplementary Fig. S1A). To investigate the nature of this short-form *p53* transcript, we performed 5′-RACE using the RLM-RACE (Ambion) kit to ensure amplifying cDNA only from full-length, capped mRNA. Two 5′-RACE products were observed when a primer derived from exon 6 was used for the 5′-RACE reaction (Fig. 5A). Sequencing analysis showed that the longer product corresponded to wild-type *p53* (data not shown). The short-form *p53* contains exons 5–12 with 155 base pairs (bp) derived from intron 4 immediately adjacent to exon 5 (Fig. 5B), suggesting that the short form is initiated from an alternative internal promoter in intron 4. The short-form transcript encodes for an N-truncated p53 protein initiated at codon 113 (named Δ113p53), and this product corresponds to Δ133p53 found in human (Bourdon et al. 2005; Supplementary Fig. S2). To further confirm that Δ*113p53* but not the wild-type *p53* is, indeed, increased in the mutant, RNA samples were prepared from wild-type embryos, from wild-type embryos injected with an effective *def* antisense morpholino (*def*-MO) (Supplementary Fig. S3), and from the *def*^{hi429} mutant embryos, respectively. RNA gel blot hybridization using probes specific for detection of wild-type *p53* (using P2 probe), Δ*113p53* (P3 probe), or both isoforms (P1 probe) showed that Δ*113p53* is, indeed, up-regulated only in the *def*^{hi429} mutant and *def*-MO morphants (Fig. 5C). Because the Δ*113p53*-specific probe is derived from the intron 4 sequence only, this result confirms the previous report that Δ*133p53* is a transcribed product initiated by the alternative promoter in intron 4 (Bourdon et al. 2005). Furthermore, quantitative real-time PCR using primer pairs specific for *p53* and Δ*113p53* showed that levels of Δ*113p53* transcripts in the mutant increased ~12-, 8.6-, and 7.7-fold at 3, 4, and 5 dpf, respectively, whereas the levels of *p53* did not show significant change between the wild type and

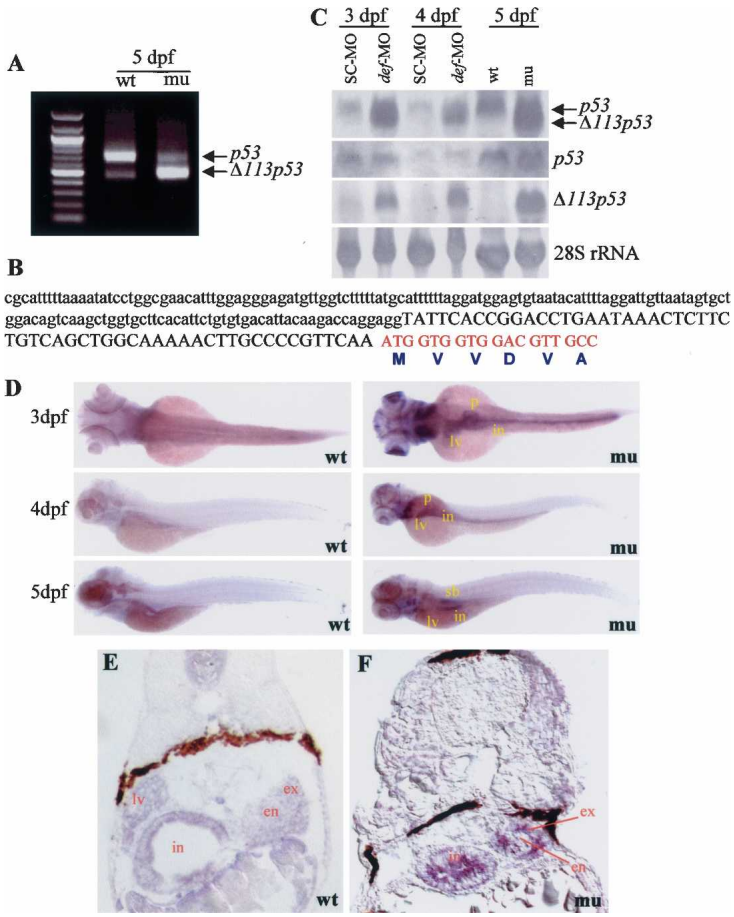

Figure 5. Loss of function of *def* selectively up-regulates the expression of Δ*113p53* in the *def*^{hi429} mutant. (*A*) 5′-RACE reaction identified two *p53* isoforms. The longer isoform corresponds to the wild-type *p53* (*p53*) and was predominant in the wild-type embryos. The short isoform (Δ*113p53*) was drastically increased in the *def*^{hi429} mutant. (*B*) The short isoform contains 155 bp derived from intron 4 (letters in lowercase) immediately adjacent to exon 5 and encodes for an N-truncated p53 protein initiated at codon 113 of the wild-type *p53*. (*C*) RNA gel blot hybridization using probes for detecting both *p53* and Δ*113p53* isoforms (P1 probe, *top* panel), *p53* only (P2 probe, second panel), and Δ*113p53* only (P3 probe, third panel) showed that Δ*113p53* but not *p53* was selectively increased in the *def*-MO morphants (*def*-MO) and *def*^{hi429} mutant (mu), respectively, when compared with the standard control MO morphants (SC-MO) and the wild-type control (wt). (*Bottom* panel) 28S rRNA was used as the loading control. (*D*) Whole-mount in situ hybridization using the P1 probe showed that Δ*113p53* expression in the *def*^{hi429} mutant (mu, *right* panels) was increased at 3 dpf, 4 dpf, and 5 dpf, and this increase was specifically limited to within digestive organs when compared with the expression of *p53* in the wild type (*left* panels). (in) Intestine; (lv) liver; (p) pancreas; (sw) swimbladder. (*E*,*F*) At 4 dpf, sectioning in situ hybridization further confirmed that *p53* expression was increased in the intestine (in), liver (data not shown), and exocrine pancreas (ex) but not in the endocrine pancreas (en) in the *def*^{hi429} mutant.

the *def*^{hi429} mutant (Fig. 6C). Taken together, our data demonstrated that loss of function of *def* selectively up-regulated the expression of Δ*113p53* but not *p53*.

Next, we investigated if the increase of Δ*113p53* is correlated to the phenotype observed in the *def*^{hi429} mutant. Whole-mount in situ hybridization using the probe detecting both *p53* and Δ*113p53* transcripts (P1 probe) showed that *p53* is ubiquitously expressed in the wild-type embryos (Fig. 5D, left panels). However, the same probe detected high levels of gene expression that appeared to be specifically restricted in the digestive organs including pharynx, liver, pancreas, and intestine in the *def*^{hi429} mutant at 3, 4, and 5 dpf, respectively (Figs. 5D [right panel], 6C; Supplementary Fig. S1B). Because molecular analyses have shown that the expression of Δ*113p53* but not *p53* was selectively elevated in the mutant (Figs. 5C, 6C) and because p53 is normally ubiquitously expressed, it is reasonable to conclude that the high levels of gene expression in the mutant digestive organs detected by the P1 probe reflected the levels of Δ*113p53*. Indeed, in situ hybridization using a Δ*113p53*-specific probe derived from intron 4 revealed that the Δ*113p53* transcripts were specifically enriched in the digestive organs (Supplementary Fig. S1C). Cross-section in situ hybridization revealed that the increase of Δ*113p53* expression is specifically within the intestinal tube, pancreas, and liver, but excluded from the islet (Fig. 5E,F), displaying a pattern closely resembled that of the *def* gene (Fig. 4G,H), which suggests that there is a strong correlation between the *def*^{hi429} mutation and the elevated Δ*113p53* expression in the digestive organs.

Knock-down of p53 *and* Δ113p53 *levels rescued mutant phenotype to normal*

Expression of Δ*113p53* was up-regulated in the *def*^{hi429} mutant, suggesting that Def might be, directly or indirectly, a negative regulator of Δ*113p53* expression and might exert its function through the p53 pathway. To answer this question, two *p53* antisense morpholinos, one specifically targeting the splicing site of exon 5 and intron 5 of the *p53* transcript (*p53*-MO^{spl}) and the other targeting the p53 start codon ATG to block the translation of p53 protein (*p53*-MO^{ATG}), were designed and injected into mutant embryos at the one-cell stage. RT–PCR showed that *p53*-MO^{spl} created aberrant splicing products in morphants (Fig. 6A). Examination of *p53*-MO^{spl} morphants 70 h post-injection using *trypsin* expression showed that the size of the mutant pancreas was restored in 24 out of 55 total mutants examined (44%) (Fig. 6B). On the other hand, only 23% of the mutants (14 out of 62 mutant embryos examined) were rescued by *p53*-MO^{ATG}. Injection of the standard control morpholino (against human β-*globin*) failed to rescue the

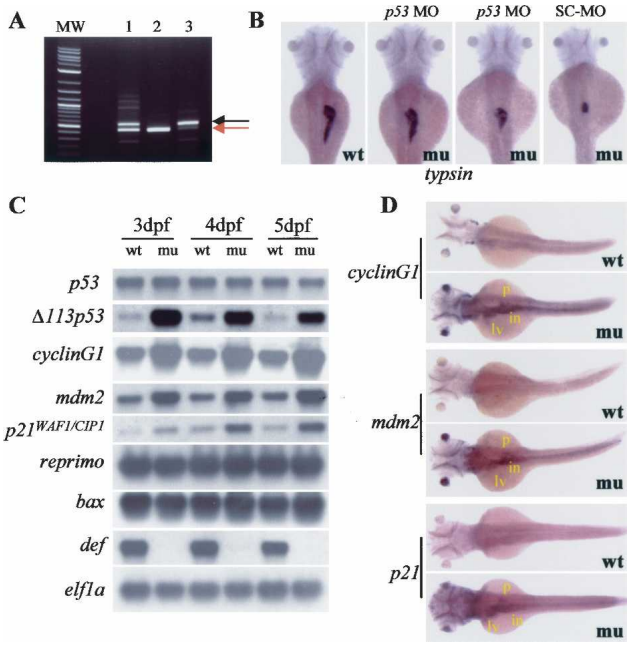

Figure 6. Cell proliferation-related but not proapoptotic-related p53 response genes are up-regulated in the *def*^{hi429} mutant. (*A*) RT–PCR analysis revealed that the *p53* MO created an aberrant product with a larger size resulting from insertion of 89 bp from the intron 5. This 89-bp insertion introduced an early stop codon in the *p53* mRNA. (MW) Molecular size marker; (lane *1*) 0.5 mM *p53* MO; (lane *2*) standard control MO (SC-MO, human β-*globin* antisense morpholinos); (lane *3*) 1.0 mM p53 MO; (red arrow) wild type *p53*; (black arrow) misspliced *p53*. (*B*) Injection of *p53*-MO^{spl} targeting *p53* mRNA rescued the mutant phenotype. Embryos 70 h post-injection were used for whole-mount in situ hybridization using a *trypsin* probe. (mu) Mutant; (wt) wild type. (*C*) Semiquantitative RT–PCR examination of expression of various p53 response genes in *def*^{hi429} mutant (mu) and the wild-type control (wt) at 3, 4, and 5 dpf, respectively. Homozygous *def*^{hi429} mutants (confirmed by lacking expression of *def*) had elevated levels of Δ*113p53*, *cyclin G1*, *p21*$^{WAF1/CIP1}$, and *mdm2* but unchanged levels of *p53*, *reprimo*, and *bax* when compared with the wild type (wt). (*D*) At 3 dpf, whole-mount in situ hybridization using *cyclin G1*, *mdm2*, and *p21*$^{WAF1/CIP-1}$ probes showed that the expression of these genes was significantly and specifically increased in the digestive organs. (in) Intestine; (lv) liver; (p) pancreas.

mutant phenotype (in a total of 59 mutant embryos examined). The *p53*-MO^{spl} morpholino is expected to knock down the levels of both *p53* and Δ*113p53* in the mutant while the *p53*-MO^{ATG} morpholino specifically targets *p53* alone. Thus, Δ*113p53* functions downstream of Def, and the elevated level of Δ*113p53* clearly contributed to the *def*^{hi429} mutant phenotype.

Elevated level of Δ113p53 *in the* def^{hi429} *mutant arrests cell proliferation rather than causing apoptosis*

Considering the fact that the initiation and early development and cell differentiation of digestive organs are relatively normal in the *def*^{hi429} mutant but not the expansion and maturation of these organs, the overall defects observed in the *def*^{hi429} mutant probably resulted from the increase of Δ*113p53* expression that leads to either arrest of cell division or an increase in apoptosis of cells within the digestive organs. We first asked if the increase in Δ*113p53* level will increase the expression of p53 response genes in the *def*^{hi429} mutant. Semiquantitative RT–PCR results showed that, in addition to Δ*113p53*, *mdm2*, and *cyclin G1*, *p21*$^{WAF1/CIP-1}$ (an inhibitor of G1-to-S-phase transition) was also up-regulated in the *def*^{hi429} mutant through 3–5 dpf (Fig. 6C). Whole-mount in situ hybridization showed that the expression of *cyclin G1*, *mdm2*, and *p21*$^{WAF1/CIP-1}$ displayed a pattern similar to that of Δ*113p53* and was specifically increased in the digestive organs in the *def*^{hi429} mutant (Fig. 6D). On the other hand, expression of *p53*, bax (apoptotic factor), and *reprimo* (G2-to-M transition-inhibiting factor) did not show discernible differences between the *def*^{hi429} mutant and the wild-type control (Fig. 6C), suggesting that the hypoplastic phenotype in the *def*^{hi429} mutant is probably not caused by increased apoptosis. In fact, the TUNEL assay did not reveal any elevated apoptotic activity in the *def*^{hi429} mutant (Supplementary Fig. S4).

A BrdU labeling experiment was performed to check the G1-to-S-phase transition. Examination of sections from wild-type embryos showed that the BrdU incorporation rate was 16.1% (504 out of 3120 total cells counted) in the liver and 15.3% (1460 out of 9548 cells counted) in the gut (Fig. 7A,C). In contrast, the incorporation rates were markedly lower in the mutant liver (10%; 244 out of 2417 cells counted) and gut (10.2%; 215 out of 2090 cells counted) (Fig. 7A,C). Next, antibody staining using anti-phosphorylated histone-3 antibody was performed to check the G2-to-M-phase transition in embryos at 3 and 4 dpf. At 3 dpf, examination of sections from wild-type embryos showed that the ratios of cells positive for phosphorylated histone-3 (P-H3) were 4.2% (144 out of 3434 cells counted) in the liver and 4% (169 out of 4173 cells counted) in the gut (Fig. 7B,D). In contrast, the ratios were significantly lower in the *def*^{hi429} mutant, with only 1.7% (26 out 1552 cells counted) in the liver and 1.6% (37 out 2303 cells counted) in the gut (Fig. 7B,D). At 4 dpf, as expected (Wallace et al. 2005), the transition from G2 to M phase slowed down in the wild type, and the ratios of cells positive for P-H3 were 2.1% (95 out 4371 cells counted) in the liver and 2.3% (199 out 8784 cells counted) in the gut. Correspondingly, the ratios of cells positive for P-H3 in the *def*^{hi429} mutant were further lowered to 0.8% (20 out of 2376 cells counted) in the liver and 0.9% (43 out of 4798 cells counted) in the gut at 4 dpf (Fig. 7B,D). Taken together, our results strongly suggest that an increase in Δ*113p53* expression causes the *def*^{hi429} mutant phenotype by arresting cell proliferation, probably through *p21* and *cyclin G1*, at the checkpoint of G1 to S or both the G1-to-S- and G2-to-M-phase transitions.

Discussion

Endoderm organogenesis includes stages of cell fate specification, bud formation, organ expansion, and cell

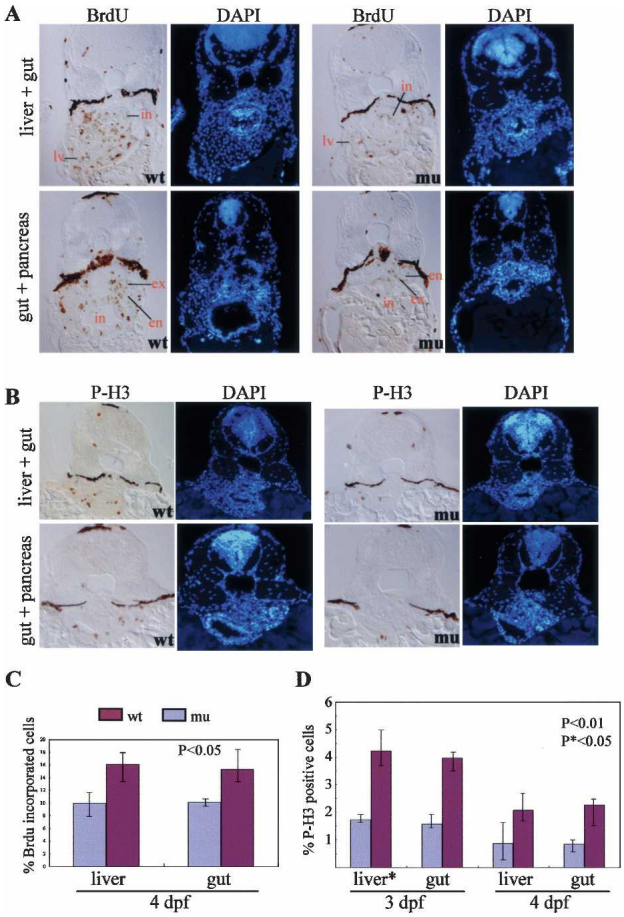

Figure 7. The *def*^{hi429} mutant phenotype is caused by compromised cell proliferation. (*A*,*C*) BrdU labeling revealed that, at 4 dpf, the number and ratio of cells entering the G1-to-S-phase transition was significantly reduced in the digestive organs of the *def*^{hi429} mutant (mu) when compared with the wild type (wt). (*Top* panel) Cross-sectioning through liver (lv) and intestine (in). (*Bottom* panel) Cross-sectioning through pancreas and intestine (in). The BrdU incorporation ratios shown in *C* were obtained by counting BrdU-labeled cells versus total cells in a specific organ (e.g., liver) in sections from seven wild-type and seven mutant embryos, respectively. (en) Endocrine pancreas; (ex) exocrine pancreas. (*B*,*D*) At 3 and 4 dpf, histochemical staining using anti-phosphorylated histone 3 (anti-P-H3) revealed that the number and ratio of cells entering G2 to M phase was drastically reduced in the digestive organs of the *def*^{hi429} mutant (mu) when compared with the wild type (wt). The ratios of P-H3-positive cells shown in *D* were obtained by counting P-H3-positive cells versus total cells in a specific organ (e.g., liver) in sections from three wild-type and three mutant embryos, respectively.

differentiation (Wells and Melton 1999; Zaret 2002). Examination of major endoderm organs including intestine, pancreas, and liver in the *def*^{hi429} mutant using organ-specific molecular markers and histological analysis showed that these organs appeared normal till 2 dpf, suggesting that *def* is not involved in or does not play a major role for the initiation and budding of digestive organs. However, digestive organs start to become hypoplastic from 3 dpf, including an underdeveloped gut tube and a smaller liver, gall bladder, pancreas, and swimbladder, whereas mesoderm-derived organs including somites, blood vessels, and pronephric ducts appeared normal. The underdevelopment of the entire digestive system in the *def*^{hi429} mutant could result from the arrest of cell differentiation as found for the *nil per ose* mutant (Mayer and Fishman 2003). If this is the case, digestive organs are probably mainly composed of progenitor cells. Although at a much lower level when compared with the wild-type control, molecular markers specific to fully differentiated intestinal epithelial cells (*ifabp* and alkaline phosphatase), hepatocytes (*lfabp* and *transferin*), and exocrine pancreas (*trypsin*) are expressed in the mutant fish, demonstrating that cell differentiation is compromised but not abolished by the *def*^{hi429} mutation. Whole-mount in situ hybridization showed that *def* expression is enriched in the entire digestive ducts and organs including pharynx, pancreas, liver, swimbladder, and intestine. Furthermore, sectioning in situ hybridization showed that *def* expression is excluded from the islet. The expression pattern of *def* perfectly matched the phenotype displayed by the *def*^{hi429} mutant and explains why the endocrine pancreas appears normal in the mutant. The evidence provided strongly suggests that Def functions as a cell-autonomous factor to regulate the expansion growth of various digestive organs except the endocrine pancreas at the later stage of endoderm organogenesis.

The *def* gene encodes a nuclear-localized novel protein. In order to study how Def controls the development of digestive organs, we compared the gene expression profiles between the *def*^{hi429} mutant and the wild-type control. As expected, the expression of a large number of enzyme genes that are known to be enriched in the intestine, liver, and pancreas is significantly decreased in the *def*^{hi429} mutant due to great loss of organ mass and compromised cell differentiation. Surprisingly, *p53* expression showed a drastic increase in the mutant embryos. Further molecular analysis revealed that Δ*113p53*, a newly identified *p53* isoform initiated from an alternative promoter in intron 4 (Bourdon et al. 2005), rather than the wild-type p53, selectively increased in the mutant. In situ hybridization showed that the increased Δ*113p53* expression is specifically limited to within the digestive organs of the mutant embryo but not in other organs. This expression pattern of Δ*113p53* in the mutant embryo phenocopies the pattern displayed by the *def* gene in the wild type, suggesting that Def might be a negative regulator of Δ*113p53* in the digestive organs and the increase in Δ*113p53* might contribute to causing the mutant phenotype. This hypothesis is supported by our data showing that injection of *p53*-MO^{spl} targeting both Δ*113p53* and *p53* exhibited a much higher rescue rate of the *def*^{hi429} mutant phenotype than did injection of *p53*-specific morpholinos *p53*-MO^{ATG}. Thus, Def functions, at least in part, through regulating the *p53* pathway to control the expansion growth of digestive organs. p53 is known to both initiate and suppress the expression of target genes to regulate cell cycle and cell death. Exami-

nation of p53 response genes showed that the expression of *p21*$^{WAF1/CIP-1}$ and *cyclin G1*, two inhibiting factors of cell proliferation (Ball 1997; Zhao et al. 2003), were increased in the *def*^{hi429} mutant. On the other hand, the expression of *bax*, a proapoptotic factor (Reed 1999), and *reprimo*, an inhibitor of G2-to-M-phase transition (Ohki et al. 2000), remained unchanged in the *def*^{hi429} mutant. These results strongly suggest that (1) Δ113p53 selectively activates the p53 response genes, and (2) the hypoplastic phenotype in the *def*^{hi429} mutant is probably due to an arrest of cell proliferation but not due to increased apoptosis. This hypothesis is further strengthened by the observation that the TUNEL assay did not reveal any obvious elevated apoptotic activities in the *def*^{hi429} mutant. In contrast, both a BrdU labeling and immunochemical staining using anti-P-H3 antibody showed that the cell division index is greatly reduced in the *def*^{hi429} mutant, demonstrating that the arrest of cell proliferation is the main cue to cause the hypoplastic phenotype in *def*^{hi429} mutant.

In zebrafish, Nodal signaling plays a decisive role in endoderm specification (Ober et al. 2003). *gata5* (Reiter et al. 1999), *hhex* (Wallace et al. 2001), *hnf1* (Sun and Hopkins 2001), *hnf6* (Matthews et al. 2004), *mnr2a* (Wendik et al. 2004), notch signaling (Lorent et al. 2004), *pdx1* (Huang et al. 2001), *prox1* (Liu et al. 2003), *ptf1a* (Lin et al. 2004), *shh* (diIorio et al. 2002), and their counterparts in other vertebrates (Edlund 2002; Zaret 2002) play crucial roles in controlling endoderm organ development in zebrafish. While some of these factors function relatively specifically only in certain endoderm organ(s) (e.g., *hhex* in liver, *pdx1* and *ptfia* in pancreas), others are known to be general factors (e.g., *shh* and notch signaling). Apparently, the final size and shape of an organ and its proper position in the body can be perfectly achieved only when the interaction of differentially expressed organ-specific factors with general factors is precisely regulated. However, little is known about the involvement of any pan-endoderm-specific factors to coordinate the expansion growth of the entire digestive system at the later stage. Here we propose that Def, like *ni per os* (Mayer and Fishman 2003), is one of such factors that acts as a pan-endoderm-specific factor to negatively regulate the expression of a general factor, namely, Δ113p53, to coordinate the proliferation of cells within digestive system. Thus, we have shown in this work that, in addition to acting as a checkpoint controller to suppress abnormal cell growth, p53 and its isoforms are closely watched and tightly controlled by organ/tissue-specific factors during organogenesis, especially at the stage wherein fast cell proliferation is needed, to prevent any adverse effect on organ/tissue growth. The remaining intriguing questions include whether Def directly or indirectly regulates Δ*113p53* expression, because currently we cannot exclude the possibility that the absence of Def could induce a generalized stress response that could indirectly up-regulate the expression of Δ*113p53*. In addition, it is also interesting to know how Δ113p53 differentially regulates the transcription of a subset of p53 response genes (e.g., *cyclin G1* and *p21*$^{WAF1/CIP-1}$) but not others (e.g., *reprimo* and *bax*). These studies provide overwhelming genetic support for the physiological significance of the newly discovered p53 isoforms and establish that they can play a key role in development. Detailed biochemical studies of these isoform interactions will be needed to understand these dramatic observations. The consequences of this new understanding of p53 function and control in development for interpreting its role in neoplasia and aging are very exciting.

Materials and methods

def^{hi429} *mutant*

Zebrafish line hi429 was obtained from a large-scale insertional mutagenesis screen using mouse retroviral vectors as the mutagen (Golling et al. 2002) and was kindly provided by Professor Nancy Hopkins at Massachusetts Institute of Technology (Cambridge, MA). Zebrafish were raised and maintained according to standard procedures (Mayer and Fishman 2003). All mutant embryos used for characterization in this report were confirmed by genotyping using two pairs of primers, one pair derived from the *LacZ* gene (P1: 5′-ATCCTCTAGACTGCCA TGG-3′; P2: 5′-ATCGTAACCGTGCATCTG-3′) harbored by the viral vector for confirmation of insertion and the other from intron II of the *def* genomic sequence (P1: 5′-TATTGCCTTAC GACAGTTT-3′; P2: 5′-CAAGCGTTTGACATTAGAGT-3′) flanking the viral vector insertion site for confirmation of the *def* gene (Fig. 3A).

Whole-mount RNA in situ hybridization

Whole-mount RNA in situ hybridizations were performed as described (Mayer and Fishman 2003). Probes were labeled with digoxigenin (DIG). *foxa1* (AL911576), *lfabp* (AL926262), *p21*$^{WAF1/CIP-1}$ (AL912410), and *p53* (AL922791) cDNA clones were from our own EST collection (Lo et al. 2003). For *transferrin* and *ifabp* (Mudumana et al. 2004), *pdx1* (NM_131443), *def* (nucleotides 336–1027), *cyclin G1* (BC052125), and *mdm2* (AF356346), primers were designed based on available sequence data, and RT–PCR products were cloned into the pGEM-T Easy Vector, respectively. Photos were taken under a Leica M216 optics.

Mutant phenotype rescue

For mRNA rescue, 1.0 ng of in vitro transcribed *def* mRNA, mutant *def*^{stop} mRNA, and *GFP* mRNA were injected into the yolk of 1-cell-stage embryos, respectively. Embryos 3 and 4 d post-injection were used for whole mount in situ. *p53*-MO^{spl} (5′-AAAATGTCTGTACTATCTCCATCCG-3′) was designed to target the splice junction between exon 5 and intron 5, and *p53*-MO^{ATG} was designed corresponding to the start codon ATG (5′-GCGCCATTGCTTTGCAAGAATTG-3′) (Langheinrich et al. 2002). Morpholinos were supplied by Gene Tools and 1 nL (0.5 mM) was injected into the yolk of one-cell-stage embryos each time. Human β-*globin* antisense morpholino (5′-CCTCTTACCTCAGTTACAATTT-3′) was used as the standard control.

Affimetrix array

Total RNA was extracted from 5 dpf wild-type and *def*^{hi429} mutant embryos, respectively, using TRIzol (GIBCO-BRL, USA) and treating with DNase I. cDNA synthesis, RNA probe label-

ing, target hybridization, washing, and staining were performed following the manufacturer's instructions (Affymetrix). GeneChip arrays were scanned on an Affymetrix probe array scanner. Data were analyzed using the statistics software MAS5.0 from Affymetrix.

Histological and immunohistochemical analysis

All embryos were anesthetized using 3-aminobenzoic acid ethyl ester, and the tail was clipped for genotyping. All photos were taken under a Zeiss Axiophot 2 optics. For hematoxylin and eosin staining, sectioning (3.5 µm) was done on paraffin-embedded embryos processed as described (Wallace et al. 2005). Embryo fixation and cryo-section in situ hybridization were performed as described (Wendl et al. 2002). For BrdU in vivo labeling, 5-bromo-2′-deoxy-uridine (BrdU) (1 nL, 10 mM; Roche) was microinjected into the peritoneal cavity of 4-dpf embryos. Embryos were incubated for 4 h at 28.5°C and then fixed at 4% PFA for 24 h before being used for immunohistochemical study as described (Wallace et al. 2005). Cells positive for P-H3 were detected using the polyclonal anti-P-H3 antibody (Santa Cruz) as the first antibody (1:200) and anti-rabbit horseradish POD (1:150) as the secondary antibody with diaminobenzidine as the substrate for color reaction. All slides were mounted with a mount medium containing DAPI (Vector). Methods for alcian blue staining and alkaline phosphatase staining were as described (Neuhauss et al. 1996; Mayer and Fishman 2003). For the nuclear-localization experiment, 1.0 ng of *def* mRNA was injected into the yolk of 1-cell-stage embryos, and embryos were collected at 10 hpf and fixed by 4% PFA at 4°C overnight and incubated with anti-Def antibody (against amino acids 32–178 raised in rabbit). Alexa Fluor 488 goat anti-rabbit IgG antibody (Molecular probes) conjugated with GFP was used as the second antibody for detection. The embryos were then deyolked and soaked in DAPI mounting medium for visualization and photography.

TUNEL assay

Cryo-sections (8 µM) were fixed in 4% PFA for 20 min, washed 30 min with PBS, and incubated in permeabilization solution (0.1% Triton X-100, 0.1% sodium citrate) for 2 min on ice. The TUNEL assay was carried out with the In Situ Cell Death Detection Kit, TMR red (Roche).

RNA gel blot hybridization, 5′-RACE, and RT–PCR

Total RNA was extracted using TRIzol (GIBCO-BRL). Poly(A)$^+$ mRNA was obtained from total RNA using the Oligotex mRNA Midi kit (QIAGEN). DIG-labeled probes (*def*: nucleotides 2108–2466; *elf1a*: nucleotides 18–706) were used for RNA gel blot hybridization as described (Wen et al. 2005). The P1 probe for detecting both *p53* and Δ*113p53* transcripts was derived from nucleotides 44–1165 of the *p53* gene. The P2 probe specific for the *p53* transcript was derived from nucleotides 7–294 of the *p53* gene, and the P3 probe specific for Δ*113p53* transcript was derived from the transcribed sequence nucleotides 13–155 originated from intron 4 (Fig. 5B). 5′-RACE was performed using the RLM-RACE kit (RNA Ligase Mediated Rapid Amplification of cDNA Ends; Ambion) according to the protocol provided by the manufacturer.

For Real-Time RT–PCR, embryos were collected at 3, 4, and 5 dpf and genotyped. RNA of individual embryos was extracted using the RNAeasy 96 kit (QIAGEN) according to the manufacturer's protocol. Ten individual wild-type and mutant embryos were pooled, respectively, and treated with DNase I. RNA was reverse-transcribed using Expand Reverse Transcriptase (Roche). The amount of transcribed cDNAs was normalized based on *elongation factor 1a* (*elf1a*) as a control with the Realtime LightCycler (Roche). The amount of template and the number of PCR cycles were optimized to ensure that the reactions were in the linear range of amplification. The primer pairs and detailed PCR conditions used to amplify each of these genes are listed in Supplementary Table 3.

Acknowledgments

We thank Professor N. Hopkins for providing the *def^{hi429}* mutant line. We thank Qi Zeng, Ke Guo, Jie Li, and Binqi Gan for histological analysis. We thank Honghui Huang, Jeremy Wu, and Lin Guo for their suggestions and technical support. This work is supported by the Agency for Science, Technology and Research in Singapore.

References

Armstrong, J.F., Kaufman, M.H., Harrison, D.J., and Clarke, A.R. 1995. High-frequency developmental abnormalities in p53-deficient mice. *Curr. Biol.* **5:** 931–936.

Ball, K.L. 1997. p21: Structure and functions associated with cyclin–CDK binding. *Prog. Cell Cycle Res.* **3:** 125–134.

Benard, J., Douc-Rasy, S., and Ahomadegbe, J.C. 2003. TP53 family members and human cancers. *Hum. Mutat.* **21:** 182–191.

Berghmans, S., Murphey, R.D., Wienholds, E., Neuberg, D., Kutok, J.L., Fletcher, C.D., Morris, J.P., Liu, T.X., Schulte-Merker, S., Kanki, J.P., et al. 2005. tp53 mutant zebrafish develop malignant peripheral nerve sheath tumors. *Proc. Natl. Acad. Sci.* **102:** 407–412.

Bourdon, J.-C., Fernandes, K., Murray-Zmijewski, F., Liu, G., Xirodimas, D.P., Saville, M.K., and Lane, D.P. 2005. p53 isoforms can regulate p53 transcriptional activity. *Genes & Dev.* **19:** 2122–2137.

Clarke, A.R., Purdie, C.A., Harrison, D.J., Morris, R.G., Bird, C.C., Hooper, M.L., and Wyllie, A.H. 1993. Thymocyte apoptosis induced by p53-dependent and independent pathways. *Nature* **362:** 849–852.

Derry, W.B., Putzke, A.P., and Rothman, J.H. 2001. *Caenorhabditis elegans* p53: Role in apoptosis, meiosis, and stress resistance. *Science* **294:** 591–595.

diIorio, P.J., Moss, J.B., Sbrogna, J.L., Karlstrom, R.O., and Moss, L.G. 2002. Sonic hedgehog is required early in pancreatic islet development. *Dev. Biol.* **244:** 75–84.

Donehower, L.A., Harvey, M., Slagle, B.L., McArthur, M.J., Montgomery Jr., C.A., Butel, J.S., and Bradley, A. 1992. Mice deficient for p53 are developmentally normal but susceptible to spontaneous tumours. *Nature* **356:** 215–221.

Edlund, H. 2002. Pancreatic organogenesis—Developmental mechanisms and implications for therapy. *Nat. Rev. Genet.* **3:** 524–532.

Field, H.A., Ober, E.A., Roeser, T., and Stainier, D.Y. 2003. Formation of the digestive system in zebrafish. I. Liver morphogenesis. *Dev. Biol.* **253:** 279–290.

Golling, G., Amsterdam, A., Sun, Z., Antonelli, M., Maldonado, E., Chen, W., Burgess, S., Haldi, M., Artzt, K., Farrington, S., et al. 2002. Insertional mutagenesis in zebrafish rapidly identifies genes essential for early vertebrate development. *Nat. Genet.* **31:** 135–140.

Greenblatt, M.S., Bennett, W.P., Hollstein, M., and Harris, C.C. 1994. Mutations in the p53 tumor suppressor gene: Clues to cancer etiology and molecular pathogenesis. *Cancer Res.*

54: 4855–4878.
Horne-Badovinac, S., Rebagliati, M., and Stainier, D.Y. 2003. A cellular framework for gut-looping morphogenesis in zebrafish. *Science* **302:** 662–665.
Huang, H., Liu, N., and Lin, S. 2001. Pdx-1 knockdown reduces insulin promoter activity in zebrafish. *Genesis* **30:** 134–136.
Jin, S., Martinek, S., Joo, W.S., Wortman, J.R., Mirkovic, N., Sali, A., Yandell, M.D., Pavletich, N.P., Young, M.W., and Levine, A.J. 2000. Identification and characterization of a p53 homologue in *Drosophila melanogaster*. *Proc. Natl Acad. Sci.* **97:** 7301–7306.
Kiefer, J.C. 2003. Molecular mechanisms of early gut organogenesis: A primer on development of the digestive tract. *Dev. Dyn.* **228:** 287–291.
Langheinrich, U., Hennen, E., Stott, G., and Vacun, G. 2002. Zebrafish as a model organism for the identification and characterization of drugs and genes affecting p53 signaling. *Curr. Biol.* **12:** 2023–2028.
Levine, A.J. 1997. p53, the cellular gatekeeper for growth and division. *Cell* **88:** 323–331.
Lin, J.W., Biankin, A.V., Horb, M.E., Ghosh, B., Prasad, N.B., Yee, N.S., Pack, M.A., and Leach, S.D. 2004. Differential requirement for ptf1a in endocrine and exocrine lineages of developing zebrafish pancreas. *Dev. Biol.* **274:** 491–503.
Liu, Y.W., Gao, W., Teh, H.L., Tan, J.H., and Chan, W.K. 2003. Prox1 is a novel coregulator of Ff1b and is involved in the embryonic development of the zebra fish interrenal primordium. *Mol. Cell Biol.* **23:** 7243–7255.
Lo, J., Lee, S., Xu, M., Liu, F., Ruan, H., Eun, A., He, Y., Ma, W., Wang, W., Wen, Z., et al. 2003. 15000 unique zebrafish EST clusters and their future use in microarray for profiling gene expression patterns during embryogenesis. *Genome Res.* **13:** 455–466.
Lorent, K., Yeo, S.Y., Oda, T., Chandrasekharappa, S., Chitnis, A., Matthews, R.P., and Pack, M. 2004. Inhibition of Jagged-mediated Notch signaling disrupts zebrafish biliary development and generates multi-organ defects compatible with an Alagille syndrome phenocopy. *Development* **131:** 5753–5766.
Matthews, R.P., Lorent, K., Russo, P., and Pack, M. 2004. The zebrafish onecut gene hnf-6 functions in an evolutionarily conserved genetic pathway that regulates vertebrate biliary development. *Dev. Biol.* **274:** 245–259.
Mayer, A.N. and Fishman, M.C. 2003. *Nil per os* encodes a conserved RNA recognition motif protein required for morphogenesis and cytodifferentiation of digestive organs in zebrafish. *Development* **130:** 3917–3928.
Melino, G., Lu, X., Gasco, M., Crook, T., and Knight, R.A. 2003. Functional regulation of p73 and p63: Development and cancer. *Trends Biochem. Sci.* **28:** 663–670.
Momand, J., Zambetti, G.P., Olson, D.C., George, D., and Levine, A.J. 1992. The mdm-2 oncogene product forms a complex with the p53 protein and inhibits p53-mediated transactivation. *Cell* **69:** 1237–1245.
Montes de Oca, L.R., Wagner, D.S., and Lozano, G. 1995. Rescue of early embryonic lethality in mdm2-deficient mice by deletion of p53. *Nature* **378:** 203–206.
Mudumana, S.P., Wan, H., Singh, M., Korzh, V., and Gong, Z. 2004. Expression analyses of zebrafish transferrin, ifabp, and elastaseB mRNAs as differentiation markers for the three major endodermal organs: Liver, intestine, and exocrine pancreas. *Dev. Dyn.* **230:** 165–173.
Neuhauss, S.C., Solnica-Krezel, L., Schier, A.F., Zwartkruis, F., Stemple, D.L., Malicki, J., Abdelilah, S., Stainier, D.Y., and Driever, W. 1996. Mutations affecting craniofacial development in zebrafish. *Development* **123:** 357–367.
Ober, E.A., Field, H.A., and Stainier, D.Y. 2003. From endoderm formation to liver and pancreas development in zebrafish. *Mech. Dev.* **120:** 5–18.
Ohki, R., Nemoto, J., Murasawa, H., Oda, E., Inazawa, J., Tanaka, N., and Taniguchi, T. 2000. Reprimo, a new candidate mediator of the p53-mediated cell cycle arrest at the G2 phase. *J. Biol. Chem.* **275:** 22627–22630.
Ollmann, M., Young, L.M., Di Como, C.J., Karim, F., Belvin, M., Robertson, S., Whittaker, K., Demsky, M., Fisher, W.W., Buchman, A., et al. 2000. *Drosophila* p53 is a structural and functional homolog of the tumor suppressor p53. *Cell* **101:** 91–101.
Reed, J.C. 1999. Dysregulation of apoptosis in cancer. *J. Clin. Oncol.* **17:** 2941–2953.
Reiter, J.F., Alexander, J., Rodaway, A., Yelon, D., Patient, R., Holder, N., and Stainier, D.Y. 1999. Gata5 is required for the development of the heart and endoderm in zebrafish. *Genes & Dev.* **13:** 2983–2995.
Sah, V.P., Attardi, L.D., Mulligan, G.J., Williams, B.O., Bronson, R.T., and Jacks, T. 1995. A subset of p53-deficient embryos exhibit exencephaly. *Nat. Genet.* **10:** 175–180.
Schumacher, B., Hanazawa, M., Lee, M.H., Nayak, S., Volkmann, K., Hofmann, R., Hengartner, M., Schedl, T., and Gartner, A. 2005. Translational repression of *C. elegans* p53 by GLD-1 regulates DNA damage-induced apoptosis. *Cell* **120:** 357–368.
Sun, Z. and Hopkins, N. 2001. vhnf1, the MODY5 and familial GCKD-associated gene, regulates regional specification of the zebrafish gut, pronephros, and hindbrain. *Genes & Dev.* **15:** 3217–3229.
Tyner, S.D., Venkatachalam, S., Choi, J., Jones, S., Ghebranious, N., Igelmann, H., Lu, X., Soron, G., Cooper, B., Brayton, C., et al. 2002. p53 mutant mice that display early ageing-associated phenotypes. *Nature* **415:** 45–53.
Vogelstein, B., Lane, D., and Levine, A.J. 2000. Surfing the p53 network. *Nature* **408:** 307–310.
Wallace, K.N. and Pack, M. 2003. Unique and conserved aspects of gut development in zebrafish. *Dev. Biol.* **255:** 12–29.
Wallace, K.N., Yusuff, S., Sonntag, J.M., Chin, A.J., and Pack, M. 2001. Zebrafish hhex regulates liver development and digestive organ chirality. *Genesis* **30:** 141–143.
Wallace, K.N., Akhter, S., Smith, E.M., Lorent, K., and Pack, M. 2005. Intestinal growth and differentiation in zebrafish. *Mech. Dev.* **122:** 157–173.
Warga, R.M. and Nusslein-Volhard, C. 1999. Origin and development of the zebrafish endoderm. *Development* **126:** 827–838.
Wells, J.M. and Melton, D.A. 1999. Vertebrate endoderm development. *Annu. Rev. Cell Dev. Biol.* **15:** 393–410.
Wen, C., Zhang, Z., Ma, W., Xu, M., Wen, Z., and Peng, J.R. 2005. Genome-wide identification of female-enriched genes in zebrafish. *Dev. Dyn.* **232:** 171–179.
Wendik, B., Maier, E., and Meyer, D. 2004. Zebrafish mnx genes in endocrine and exocrine pancreas formation. *Dev. Biol.* **268:** 372–383.
Wendl, T., Lun, K., Mione, M., Favor, J., Brand, M., Wilson, S.W., and Rohr, K.B. 2002. Pax2.1 is required for the development of thyroid follicles in zebrafish. *Development* **129:** 3751–3760.
Zaret, K.S. 2002. Regulatory phases of early liver development: Paradigms of organogenesis. *Nat. Rev. Genet.* **3:** 499–512.
Zhao, L., Samuels, T., Winckler, S., Korgaonkar, C., Tompkins, V., Horne, M.C., and Quelle, D.E. 2003. Cyclin G1 has growth inhibitory activity linked to the ARF-Mdm2-p53 and pRb tumor suppressor pathways. *Mol. Cancer Res.* **1:** 195–206.

Loss of function of *def* selectively up-regulates Δ*113p53* expression to arrest expansion growth of digestive organs in zebrafish

Jun Chen, Hua Ruan, Sok Meng Ng, et al.

Genes Dev. 2005, **19:**
Access the most recent version at doi:10.1101/gad.1366405